Kinetic Study and Theoretical Analysis of Hydroxyl Radical Trapping and Spin Adduct Decay of Alkoxycarbonyl and Dialkoxyphosphoryl Nitrones in Aqueous Media

Frederick A. Villamena,† Christopher M. Hadad,‡ and Jay L. Zweier*,†

Center for Biomedical EPR Spectroscopy and Imaging, The Davis Heart and Lung Research Institute, College of Medicine, and Department of Chemistry, The Ohio State University, Columbus, Ohio 43210

Received: December 26, 2002; In Final Form: March 21, 2003

Spin-trap development is important because of limitations that still exist among the currently used nitrone spin traps. This study correlates the experimental kinetic data with theoretical calculations, a novel approach that could be helpful in the future design of new spin traps. The kinetics of hydroxyl radical (•OH) trapping and spin adduct decay of the alkoxycarbonyl-nitrones 5-ethoxycarbonyl-5-methyl-1-pyrroline *N*-oxide (EMPO) and 5-butoxycarbonyl-5-methyl-1-pyrroline *N*-oxide (BocMPO) as well as the dialkoxyphosphoryl-nitrones 5-diethoxyphosphoryl-5-methyl-1-pyrroline *N*-oxide (DEPMPO) and 5-diisopropyloxyphosphoryl-5-methyl-1-pyrroline *N*-oxide (DIPPMPO) have been investigated and compared with those of unsubstituted 5,5-dimethyl-1-pyrroline *N*-oxide (DMPO). Kinetic investigation was performed by the steady-state generation of •OH from H_2O_2 by UV photolysis in the presence of a nitrone. Apparent rate constants of •OH trapping by EMPO, BocMPO, DEPMPO, and DIPPMPO in competition with ethanol are all comparable, with k_{app} values ranging from 4.99 ± 0.36 to 4.48 ± 0.32 M^{-1} s^{-1} and the commonly used spin trap 5,5-dimethyl-1-pyrroline *N*-oxide (DMPO) having a lower k_{app} of 1.93 ± 0.05 M^{-1} s^{-1}. Half-lives of the •OH adducts of EMPO, DEPMPO, and DIPPMPO are much longer ($t_{1/2} = 127-158$ min) than those of DMPO and BocMPO with half-lives of only 55 and 37 min, respectively. Geometry optimizations, frequency analyses, and single-point energies of the nitrones and their corresponding spin adducts were determined at the B3LYP/6-31G*//HF/6-31G* level to rationalize the experimental results.

Introduction

The detection of transient radicals has relied strongly on the electron paramagnetic resonance (EPR) method by spin trapping using nitrone spin traps. Spin trapping has increased in importance for understanding the reaction kinetics and mechanisms of certain organic reactions,[1−4] sonolysis,[5] lipid peroxidation,[6−8] smoke toxicity,[9] Fenton-type reactions,[10,11] and in vivo and in vitro enzymatic reactions.[12−15] The role of reactive oxygen species (ROS) such as hydroxyl (•OH) or superoxide ($O_2^{\bullet-}$) radicals in physiological and pathological processes has been extensively studied.[16−19]

Several limitations in both the chemical and physical properties of these spin traps still exist. These disadvantages include the instability of generated radical adducts, which affects the accurate characterization and quantification of radicals formed in biological reactions, a lack of specificity to certain types of radicals, and difficulty in purification of the spin trap that oftentimes leads to contamination by paramagnetic species. The design of new spin traps faces several challenges that include the efficiency of radical trapping, ease of handling, long shelf life, and minimized cytotoxicity of the spin trap as well as long half-lives for the radical adducts formed. Several nitrones have been previously evaluated for •OH trapping. Among these traps were β-phosphorylated[20−23] PBN-type **1** and cyclic nitrones **2**, 5-butyl-5-methyl-1-pyrroline *N*-oxides[24] **3**, imidazole *N*-oxides[25] **4**, and 5-carboxy-5-methyl-1-pyrroline *N*-oxide[26] **5**.

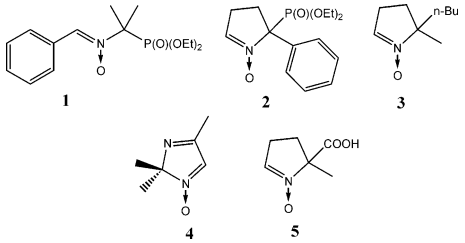

Although it has been demonstrated using Fenton chemistry or the UV photolysis of H_2O_2 that these nitrones trap the •OH radical, some of these nitrones are limited by their commercial availability. In this paper, we used the formation of the •OH spin adduct as a model to evaluate the trapping efficiency and adduct stability of the commercially available nitrones DMPO, EMPO, DEPMPO, and DIPPMPO, which are all commonly used in in vivo as well as in vitro applications. Although there have been important published reports about the spin-trapping characteristics of the commercially available nitrone spin traps[27−31] used in this study, kinetic data on the •OH trapping and decay of the •OH adduct of some of these nitrones has not been reported and systematically compared. Theoretical studies at the B3LYP/6-31G(d)//HF/6-31G(d) level of theory were used to rationalize the spin-trapping efficiency and spin adduct stability of nitrones and nitroxides, respectively. These analyses will be very useful for the design of new spin-trapping agents of enhanced synthetic and biological utility.

* Corresponding author. E-mail: zweier-1@medctr.osu.edu. Tel: (614)-247-7857. Fax: (614)-247-7845.

† Center for Biomedical EPR Spectroscopy and Imaging and The Davis Heart and Lung Research Institute.

‡ Department of Chemistry.

10.1021/jp027829f CCC: $25.00 © 2003 American Chemical Society
Published on Web 05/09/2003

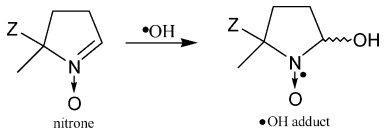

nitrone	Z
DMPO	-Me
EMPO	$-CO_2Et$
BocMPO	$-CO_2$*t*-Bu
DEPMPO	$-P(O)(OEt)_2$
DIPPMPO	$-P(O)(O$*i*$-Pr)_2$

We herein report the kinetics of •OH trapping by some nitrones and the decay of their corresponding spin adducts and correlation of these experimental results with theoretical calculations at the B3LYP/6-31G*//HF/6-31G* level of theory.

Experimental Section

Nitrones. Nitrones EMPO, DEPMPO, and DIPPMPO (Oxis-Research, Oregon) and DMPO (Dojindo Labs, Japan) were used as purchased without further purification. BocMPO was prepared on the basis of the procedure described by Zhao et al.[30] with minor modifications as described elsewhere.[32] Nitrone BocMPO, mp 94−95 °C, δ_H (200 MHz; $CDCl_3$; Me_4Si): 1.49 (9H, s, *t*-Bu), 1.67 (3H, s, C(5)Me), 2.10−2.16 and 2.51−2.59 (2H, m, C(4)H), 2.80−2.64 (2H, m, C(3)H), 6.98 (1H, s, C(2)H). Hydrogen peroxide H_2O_2 was purchased from Acros Organics as a 35% w/w solution. Ethanol (Pharmco, CT) was 99.96% ACS/USP grade.

EPR Measurements. EPR measurements were carried out on a Bruker EMX-X band spectrometer with an HS resonator at room temperature. General instrument settings are as follows unless otherwise noted: microwave power, 10 mW; modulation amplitutude, 1.0 G; receiver gain, 3.17−3.56 × 10^5 ; for field sweep: scan time, 168 s; time constant, 328 ms; for time scan: scan time 335−2680 s; time constant, 1310 ms. Measurements were performed in an AquaX flow-through sample cell. Simulations were made using the EPR Data Analysis Program (EPRDAP) version 2.0 written by Professor P. Kuppusamy.

Competitive Spin Trapping. All kinetic experiments were performed using Dulbelcco's phosphate-buffered saline (Gibco) containing 0.1 mM diethylenetriaminepentaacetic acid (DTPA) as an iron chelator. The hydroxyl radical (•OH) was generated by the UV photolysis of H_2O_2. All solutions were bubbled with nitrogen gas prior to irradiation. The sample cell was irradiated with a Spectroline low-pressure mercury vapor lamp with 0.64 cm × 5.4 cm dimensions and a 254-nm wavelength. In a typical competitive spin-trapping experiment, a 400-μL solution contained 25 mM of the nitrone, 1.3 mM H_2O_2, and varying amounts of EtOH (0−75 mM) or, in some cases, 50 mM nitrone with 0−150 mM EtOH. The mixture was transferred to a 1-mL syringe and injected into the AquaX sample cell. Kinetic measurements began when the power source was turned on. The growth of either the first or second low-field peaks was monitored as a function of time over a period of 335 s. All data were the average of three or more measurements. For all spin adducts, spectra were taken after each irradiation, and the final intensities of either the first or second peaks are reproducible with a standard deviation of only 10%, whereas peak positions have a deviation of less than 0.3 G. The average intensity ratio ($I_{\text{first peak}}/I_{\text{second peak}}$) in the absence and presence of EtOH (1, 1.5, 2, and 3 equiv) has a standard deviation of less than 7%.

Decay Kinetics. In a typical kinetic decay study, 400 μL of a solution contains 50 mM nitrone and 330 μM H_2O_2. The mixture was injected into the sample cell and irradiated for 3 min. The first or second low-field peak decay was monitored as a function of time over a period of 2680 s after the light source was turned off. All data were the average of three or more measurements. The reproducibility of peak intensities after 3 min of irradiation is reasonable with a standard deviation of less than 10%.

Theoretical Calculations. Hartree−Fock (HF) theory[33] was applied in this study to determine the optimized geometry and vibrational frequencies for each intermediate, whereas density functional theory[34,35] (DFT) was used for single-point energies

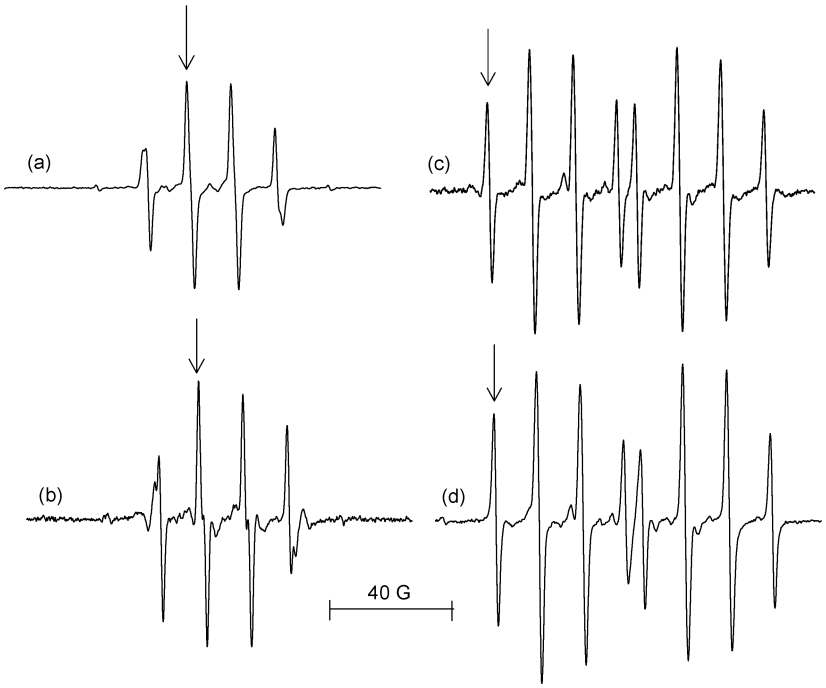

Figure 1. EPR spectral profiles of (a) EMPO/•OH, (b) BocMPO/•OH, (c) DEPMPO/•OH, and (d) DIPPMPO/•OH. Spectra were taken from 25 mM nitrone, 1.3 mM H_2O_2 with UV irradiation. All spectra were scaled on the same $x-y$ coordinate range. Arrows indicate the peak that is being monitored. See Experimental Section for spectrometer settings.

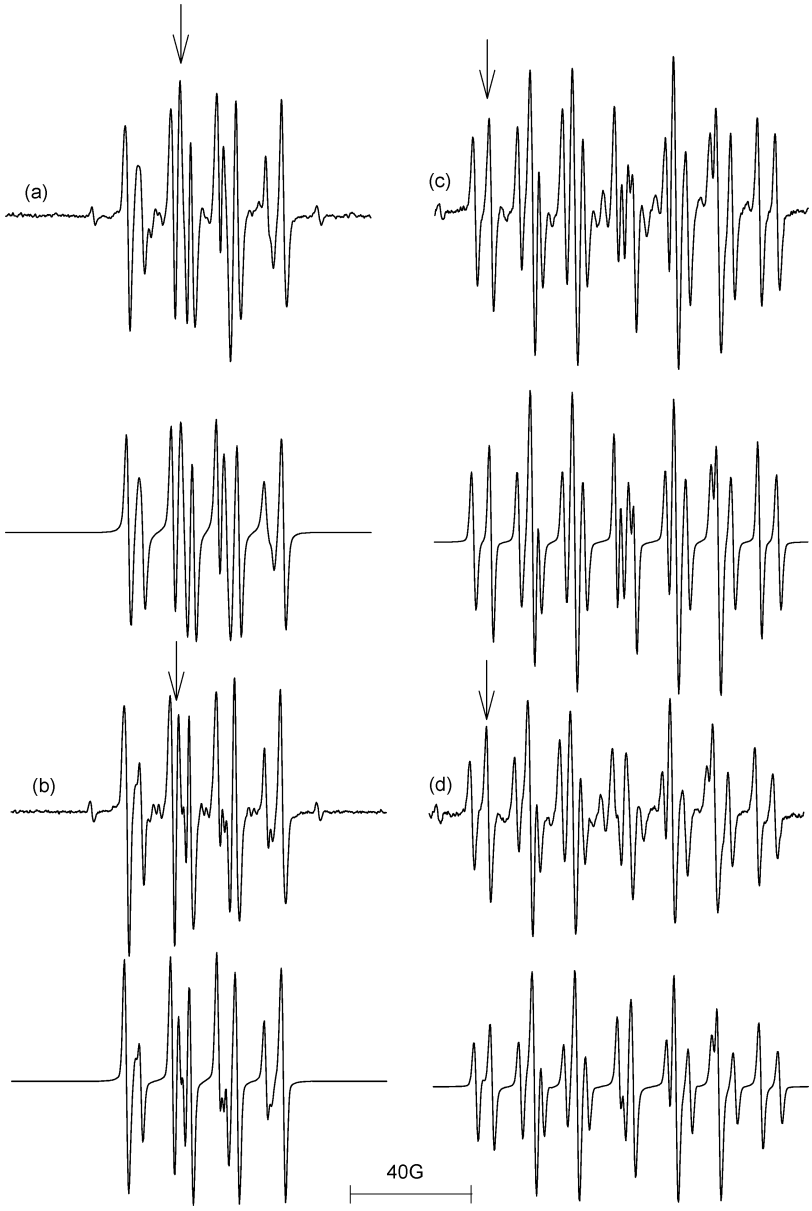

Figure 2. EPR spectral profiles of (a) EMPO/•OH, (b) BocMPO/•OH, (c) DEPMPO/•OH, and (d) DIPPMPO/•OH in the presence of the α-hydroxy-ethyl radical adduct. Below each spectrum is its respective simulated spectrum. Spectra were taken from 25 mM nitrone, 75 mM EtOH, 1.3 mM H_2O_2 upon UV irradiation. All spectra were scaled on the same $x-y$ coordinate range. Arrows indicate the peak that is being monitored. See Experimental Section for spectrometer settings.

of all of the stationary points.[33,36−38] All calculations were performed using Gaussian 98[39] at the Ohio Supercomputer Center. Starting conformations for the carboxylated and phosphorylated nitrones were based on the reported X-ray structures for 2-(diethoxyphosphoryl)-2-phenethyl-3,4-2H-pyrrole-1-oxide (DEPPEPO)[40] and BocMPO,[41] respectively. Single-point energies were obtained at the B3LYP/6-31G* level with the optimized HF/6-31G* geometries. Stationary points for both the nitrone spin traps and •OH adducts were found to be energy minima via vibrational frequency analysis (HF/6-31G*) in which there were no imaginary vibrational frequencies, and zero-point vibrational energies (ZPE) were scaled by a factor of 0.9135.[42] Attempts to locate the transition state (by using the opt=ts,calcfc command) on the partially optimized structures failed. Spin contamination for all of the stationary point for the •OH adduct structures was minimal (i.e., $0.76 < \langle S^2 \rangle < 0.77$). All charge densities were obtained using natural population analysis (NPA) at the HF/6-31G* level.[43]

Results and Discussion

Kinetics of Hydroxyl Radical Trapping. Figure 1 shows representative spectra of the •OH adducts of various alkoxycarbonyl and dialkoxyphosphoryl nitrones during UV irradiation in the presence of H_2O_2. The formation of spin adduct artifacts was minimal compared to that of the •OH adducts. Rate constants for the •OH trapping of DMPO, EMPO, BocMPO, DEPMPO, and DIPPMPO were determined in competition with EtOH. Figure 2 shows representative spectra of adducts BocMPO/•OH and DEPMPO/•OH in competition with EtOH showing the α-hydroxy-ethyl radical CH_3•CHOH adduct. Table 1 shows the simulated spectral data of •OH and CH_3•CHOH adducts in which no serious overlap occurred between the two adducts. There was no significant shift in the peak positions of the first and second low-field peaks (which hereafter will be referred to simply as the first and second peaks, respectively) after irradiation both in the presence and absence of EtOH. Moreover, the ratio of peak height intensities between the first

TABLE 1: EPR Parameters of Simulated •OH and α-Hydroxy-Ethyl Radical Adducts

adducts	diastereomers (%)[a]	hyperfine coupling constants (G)			
		A_N	A_H^β	A_H^γ	A_P
DMPO/•OH	100	14.90	14.9		
EMPO/•OH	66	14.50	14.5	1.2	
	34	14.00	13.0		
BocMPO/•OH	44	14.50	14.2	1.2	
	56	14.20	12.5		
DEPMPO/•OH	37	13.90	13.0	0.27(3H)	47.3
	63	13.90	12.5	0.27(3H)	47.3
DIPPMPO/•OH	62	14.07	13.5	0.27(3H)	46.5
	38	14.07	12.6	0.27(3H)	46.5
DMPO/CH_3•CHOH	100	15.96	23.0		
EMPO/CH_3•CHOH	54	15.09	22.0		
	46	15.40	21.5		
BocMPO/CH_3•CHOH	39	15.13	21.4		
	61	15.13	22.4		
DEPMPO/CH_3•CHOH	40	14.95	22.6		48.8
	60	14.95	21.6		48.8
DIPPMPO/CH_3•CHOH	65	14.73	21.8		48.5
	35	14.60	21.5		48.5

[a] For the α-hydroxy-ethyl radical adducts, simulation is based on the spectrum in the presence of the •OH adduct.

and second peaks remained constant throughout the experiment, indicating that the C-centered α-hydroxy-ethyl radical adduct spectra does not interfere with the spectra of the •OH adduct. Peak height intensities of the first peak were monitored for adducts DMPO/•OH, DEPMPO/•OH, and DIPPMPO/•OH. Two maxima at the first peak were evident for EMPO/•OH and BocMPO/•OH (see Figure 3a−d), corresponding to the diastereomeric species formed. Only the second peak was monitored for EMPO/•OH and BocMPO/•OH (see Figure 1a and b) because the first peak has an irregular shape, and the relative intensities of the two maxima constantly changed during the course of irradiation and were affected by the amount of EtOH present.

The hydroxyl radical was generated at a steady-state condition. Peak height intensities of the first or the second peaks were monitored for approximately 5 min. Peak growth is linear during the first 3 min of irradiation and then begins to deviate from linearity thereafter. Figure 4 shows the inhibition of the DEPMPO/•OH adduct formation in the presence of varying amounts of EtOH. With all of the spin traps studied here, only minor peak growth was observed upon irradiation of the spin trap by itself. However, this growth was much less than that when H_2O_2 was present. Because the amount of spin trap is constant throughout the experiments with only the amount of EtOH being varied, the formation of this adduct due to irradiation alone (in the absence of H_2O_2) will be a constant factor and should average out any error that may arise from it.

The increase in peak intensity of the first or second peak was monitored, and the initial rates of formation were determined within 50−150 s, in which the earliest linear curve becomes evident. Data were plotted using eq 1

$$\frac{V}{\nu} - 1 = \frac{k_{\mathrm{EtOH}}[\mathrm{EtOH}]}{k_{\mathrm{nitrone}}[\mathrm{nitrone}]} \qquad (1)$$

where V and ν are the initial rates of •OH adduct formation in the absence and presence of EtOH, respectively; k_{EtOH} and k_{nitrone} are the second-order rate constants of EtOH and the nitrone spin trap, respectively; and [EtOH] and [nitrone] are concentrations. Table 2 shows the rate constants of •OH trapping by various nitrones in competition with EtOH on the basis of an

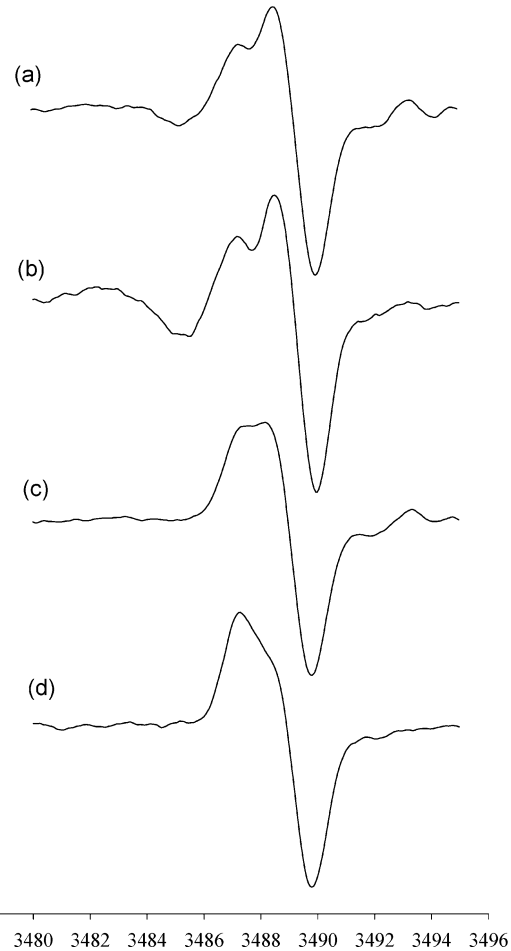

Figure 3. Relative formation and decay of the low-field peak with two maxima corresponding to the cis−trans isomers (a) during 5 min of UV irradiation of BocMPO in the presence 1.3 mM H_2O_2 and (b) 25 min after the UV lamp was turned off. Spectra (c) and (d) are the same as (a) and (b), respectively, but using nitrone EMPO.

assumed k_{EtOH} value[44] of 1.8×10^9 M^{-1} s^{-1}. Apparent rate constant values for nitrones EMPO, BocMPO, DEPMPO, and DIPPMPO range from $\{4.59(22)-4.99(36)\} \times 10^9$ M^{-1} s^{-1} and are within experimental error except for DMPO, where $k_{\mathrm{DMPO}} = 1.93(5) \times 10^9$ M^{-1} s^{-1}. Several rate constants have been reported for •OH trapping by DMPO using different •OH generating systems[45] ranging from $(2-5.2) \times 10^9$ M^{-1} s^{-1}. However, Finkelstein et al.[31] reported a value of $k_{\mathrm{DMPO}} = 3.4 \times 10^9$ M^{-1} s^{-1} by UV photolysis and a value of 2.1×10^9 M^{-1} s^{-1} by the Fenton reaction. The k_{app} value of 2.1×10^9 M^{-1} s^{-1} derived from the Fenton reaction is closer to the value derived from our study using UV photolysis. Moreover, Frejaville et al.[29] reported a k_{DEPMPO} value from the Fenton reaction of 7.8×10^9 M^{-1} s^{-1}, which is based on $k_{\mathrm{DMPO}} = 3.4 \times 10^9$ M^{-1} s^{-1} reported by Finkelstein using UV photolysis. A ratio of literature values for $k_{\mathrm{DMPO}}/k_{\mathrm{DEPMPO}} = 3.4 \times 10^9/7.8 \times 10^9$ M^{-1} $s^{-1} = 0.44$ can be obtained, whereas our study gives a ratio for $k_{\mathrm{DMPO}}/k_{\mathrm{DEPMPO}}$ of $1.93(5) \times 10^9/4.83(36) \times 10^9$ M^{-1} $s^{-1} = 0.40$, which is within the experimental error of the value observed by Frejaville et al.[29]

The hydroxyl radical responds randomly to polar substituent effects because of its high reactivity, especially with polarized double bonds. This electrophilic nature[46] of •OH as demonstrated by its high reactivity to electron-rich centers such as the nitrone functionality accounts for the small differences in rate constants among the substituted nitrones. Although all of the rate constants are within diffusion-controlled values, the 2-fold difference in

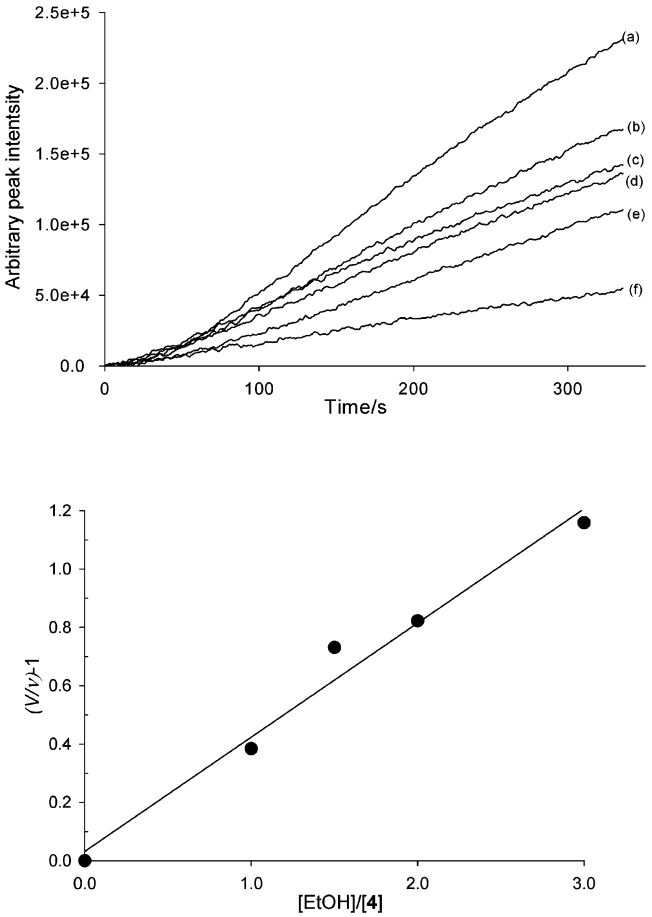

Figure 4. (Top) Low-field peak formation during competitive trapping of 25 mM DEPMPO with (a) 0 mM, (b) 25 mM, (c) 37.5 mM, (d) 50 mM, and (e) 75 mM EtOH in the presence of 1.3 mM H_2O_2. Plot (f) contains only 25 mM of DEPMPO with no H_2O_2 or EtOH added. (See Experimental Section for the parameters that were used.) (Bottom) Typical plot of $V/\nu - 1$ vs [EtOH]/[DEPMPO] using the data shown above.

TABLE 2: Apparent Rate Constants for the Spin Trapping of Hydroxyl Radicals by Various Nitrones[a]

Spin Trap

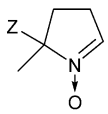

Z=	rate constants[b] ($k_{app}/10^{-9}$ M^{-1} s^{-1})	ref
$-CH_3$ (DMPO)	1.93 ± 0.05	this work
	2.1[c]	31
	3.4[d]	31
$-CO_2Et$ (EMPO)	4.99 ± 0.36	this work
$-CO_2t$-Bu (BocMPO)	4.48 ± 0.32	this work
$-P(O)(OEt)_2$ (DEPMPO)	4.83 ± 0.34	this work
	7.8[c]	28,29
$-P(O)(O\mathit{i}\text{-Pr})_2$ (DIPPMPO)	4.59 ± 0.22	this work

[a] At 25 °C in pH 7.2 phosphate buffer by UV photolysis of nitrone in competition with EtOH in the presence of H_2O_2. [b] Values based on three to four measurements with $r^2 = 0.98-99$. [c] Fenton reaction. [d] UV photolysis with H_2O_2.

the rate constants of the substituted nitrones compared to that of DMPO is significant because this can offer several advantages in terms of higher signal intensity or the use of lower concentrations for spin trapping.

Theoretical analysis was performed at the B3LYP/6-31G*//HF/6-31G* level to rationalize the difference in favorability in the formation of substituted nitrones/•OH adducts versus the DMPO/•OH adduct. The addition of •OH to all of the nitrones is exothermic (see Table 3), with ΔE_{rxn} ranging from −58.6 to −61.1 kcal/mol with the formation of phosphorylated •OH adducts being the most exothermic followed by the carboxylated nitrones and DMPO being the least exothermic. These ΔE_{rxn} values are within the range reported by Boyd and Boyd[47] for the barrierless •OH addition to $CH_2{=}NH(O)$ of −244 kJ/mol or −58.3 kcal/mol at the MP2/6-31+G**//HF/6-31G* level of theory. An examination of the relative ΔH_{rxn} at 298 K (Table 3) shows that the heats of reaction for the formation of substituted spin adducts are more exothermic than for DMPO/•OH. In the case of carboxylated nitrones EMPO and BocMPO, there is no preference in the formation of either the cis or trans configuration as shown by the relative ΔH_{rxn} in Table 3, whereas the cis configuration is preferred for both the phosphorylated nitrones DEPMPO and DIPPMPO by about 2.4 kcal/mol, which is exothermic relative to the formation of DMPO−OH. This highly favorable formation of the cis isomer compared to the formation of DMPO and carboxylated nitrone •OH adducts can be rationalized by the presence of intramolecular H-bonding between the phosphoryl-O and the hydroxyl-H in the optimized structures (see Scheme 1). The H-bond distance was predicted to be around 2.03Å for •OH adducts with both DEPMPO and DIPPMPO. In addition, calculations were performed on the carboxylated nitrone •OH adduct structures similar to those of the phosphorylated •OH adducts with intramolecular H-bonding. (Data are not included in Table.) The predicted H-bond distance between the carbonyl-O and hydroxyl-H for both EMPO and BocMPO •OH adducts is about 2.17 Å longer than that for the DEPMPO and DIPPMPO •OH adducts. ΔH_{rxn} for the formation of EMPO and BocMPO •OH adducts with intramolecular H-bonding is only about 0.4 kcal/mol more exothermic than the formation of their respective trans isomers compared to the values for DEPMPO and DIPPMPO, which are about 2.1 and 5.9 kcal/mol, respectively. Relative ΔG_{rxn} energies also gave a similar pattern to the ΔH_{rxn} values in which the formation of either cis or trans isomers for carboxylated adducts and the cis isomers for the phosphorylated adducts (DEPMPO/•OH and DIPPMPO/•OH) is thermodynamically favored. A general trend is noticeable in which the preferred •OH adduct isomers are more polar than the less preferred configurations as shown by their dipole moments (Table 3).

The similarities in k_{app} of •OH trapping for EMPO, BocMPO, DEPMPO, and DIPPMPO despite the significant differences in the charges of the nitronyl-C, which is the site of •OH addition in EMPO (0.008), BocMPO (0.010), DEPMPO (0.033), and DIPPMPO (0.023) (see Table 4), demonstrate the highly electrophilic character of •OH. However, the negatively charged nitronyl-C in DMPO (−0.008) may have a significant contribution to its relatively lower reactivity toward •OH compared to the substituted nitrones. This indicates that the rate of •OH trapping can be influenced by the charge on the nitronyl-C as well, despite the high reactivity of •OH. This is in agreement with a previous report on $O_2^{\bullet-}$ trapping[32] by nitrones DMPO, BocMPO, and DEPMPO in which the rate of trapping was also affected significantly by small difference in atomic charge at C-2. The superoxide radical, being a negatively charged radical, is more nucleophilic than •OH and is therefore even more sensitive to the atomic charge on C-2.

Kinetics of the Decay of Hydroxyl Radical Adducts. The intensities of the first or second peaks were monitored, normal-

TABLE 3: Reaction Energies in Theoretically Optimized Structures of Nitrones and Spin Adducts at the B3LYP/6-31G*//HF/6-31G* Level[a]

	ΔE_{rxn}[b]		ΔH_{rxn}[e]		ΔG_{rxn}[f]		
spin adducts	absolute[c]	relative[d]	absolute	relative	absolute	relative	dipole[g]
DMPO/•OH	−58.6	0.0	−55.2	0.0	−45.3	0.0	2.47
EMPO/•OH (cis)	−59.3	−0.8	−56.0	−0.9	−46.7	−1.5	2.56
EMPO/•OH (trans)	−59.8	−1.2	−56.4	−1.2	−46.8	−1.5	2.99
BocMPO/•OH (cis)	−59.3	−0.7	−55.9	−0.8	−45.9	−0.6	2.55
BocMPO/•OH (trans)	−59.4	−0.8	−55.9	−0.8	−46.0	−0.7	2.96
DEPMPO/•OH (cis)	−61.2	−2.6	−57.5	−2.4	−46.9	−1.6	4.34
DEPMPO/•OH (trans)	−58.9	−0.4	−55.5	−0.3	−45.8	−0.5	1.87
DIPPMPO/•OH (cis)	−61.1	−2.5	−57.5	−2.4	−46.9	−1.7	4.94
DIPPMPO/•OH (trans)	−55.1	3.4	−51.9	3.5	−43.0	2.3	4.54

[a] See Experimental Section for the calculation procedure employed. [b] ΔE_{rxn} (kcal/mol) = ΔE_{tot}(spin adduct) − ΔE_{tot}(spin trap + •OH). [c] Based on the bottom-of-the-well energy. [d] Relative values are energies of reactions relative to DMPO/•OH. [e] ΔH_{rxn} (kcal/mol) = ΔH(spin adduct) − ΔH(spin trap + •OH) at 298 K. [f] ΔG_{rxn} (kcal/mol) = ΔG(spin adduct) − ΔG(spin trap + •OH) at 298 K. [g] In debye.

TABLE 4: Natural Charges of Nitronyl-Nitrogen, −Oxygen, C-2, and C-5 in HF/6-31G*-Optimized Nitrones and Their •OH Spin Adducts Using Natural Population Analysis[a]

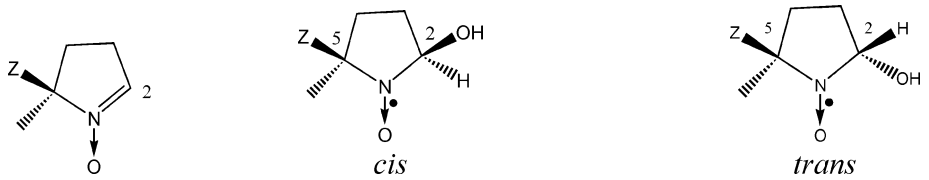

		cis				trans			
adducts	C-2	N	O	C-2	C-5	N	O	C-2	C-5
$-CH_3$ (DMPO)	−0.008	0.001	−0.417	0.253	0.103				
$-CO_2Et$ (EMPO)	0.008	0.006	−0.411	0.258	0.016	0.001	−0.402	0.251	0.013
$-CO_2t$-Bu (BocMPO)	0.010	0.008	−0.413	0.258	0.017	0.003	−0.405	0.251	0.015
$-P(O)(OEt)_2$ (DEPMPO)	0.033	−0.015	−0.392	0.250	−0.280	−0.001	−0.415	0.252	−0.283
$-P(O)(O\textit{i}\text{-}Pr)_2$ (DIPPMPO)	0.023	−0.021	−0.382	0.250	−0.275	−0.024	−0.378	0.253	−0.273

[a] At the HF/6-31G* level. NPA analysis for OH radical: −0.414 (O) and 0.414 (H).

SCHEME 1

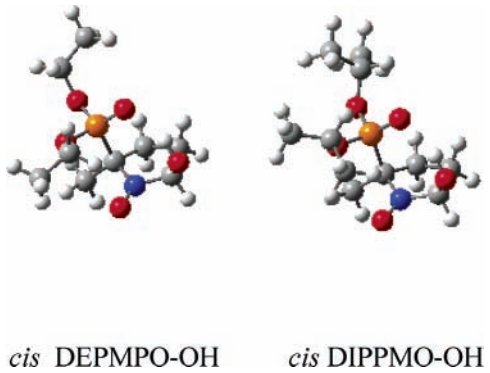

ized, and plotted over a period of approximately 45 min after the UV light was turned off. Peak intensities of paramagnetic species due to the irradiation of the nitrone alone are very minimal (<2%) compared to the •OH adduct peak intensity, and no overlap was observed between the two species. Figure 5 shows representative decay plots of all of the •OH adducts. Evident from the plots is that the decay of both DMPO/•OH and BocMPO/•OH adducts is relatively faster than that of the EMPO/•OH, DEPMPO/•OH, and DIPPMPO/•OH spin adducts. An analysis of the decay plots for all adducts did not fit either pure first or second order alone. First-order plots begin to deviate from linearity after 5−10 min. Therefore, a more complicated rate equation (eq 2) involving simultaneous unimolecular and bimolecular decay is employed,

$$-\frac{d[\text{adduct}]}{dt} = k_1[\text{adduct}] + 2k_2[\text{adduct}]^2 \qquad (2)$$

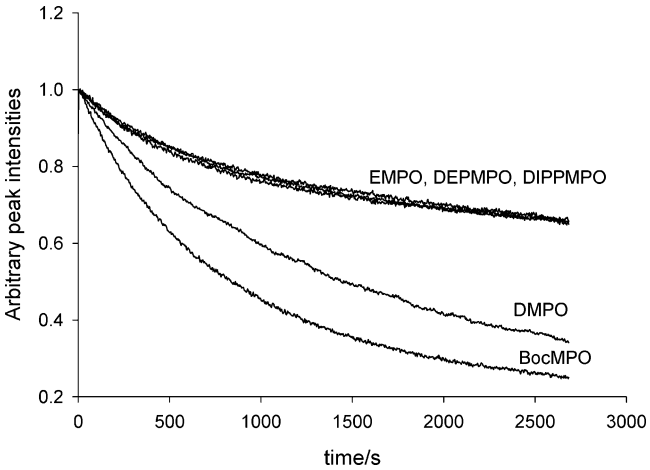

Figure 5. Decay plots of •OH adducts of DMPO, EMMPO, BocMPO, DEPMPO, and DIPPMPO after 3 min of UV irradiation of solutions containing the corresponding nitrone (50 mM) and H_2O_2 (330 μM) in pH 7.0 phosphate buffer.

in which [adduct] is the concentration of •OH adducts and k_1 and k_2 are the first- and second-order rate constants, respectively. Rate constant k_1 was derived independently and was based on the latter part of the decay plot that is usually between 25 and 45 min. These values were used to fit the decay plots using the integrated form of eq 2 in which $k_2[\text{adduct}]_o$ values were also calculated. Because of the persistence of the EMPO/•OH, DEMPO/•OH, and DIPPMPO/•OH spin adducts (with only less than 70% of the initial spin adducts having decomposed), k_1 values can therefore be overestimations of the actual values. Table 5 shows the kinetic data derived from such plots. The

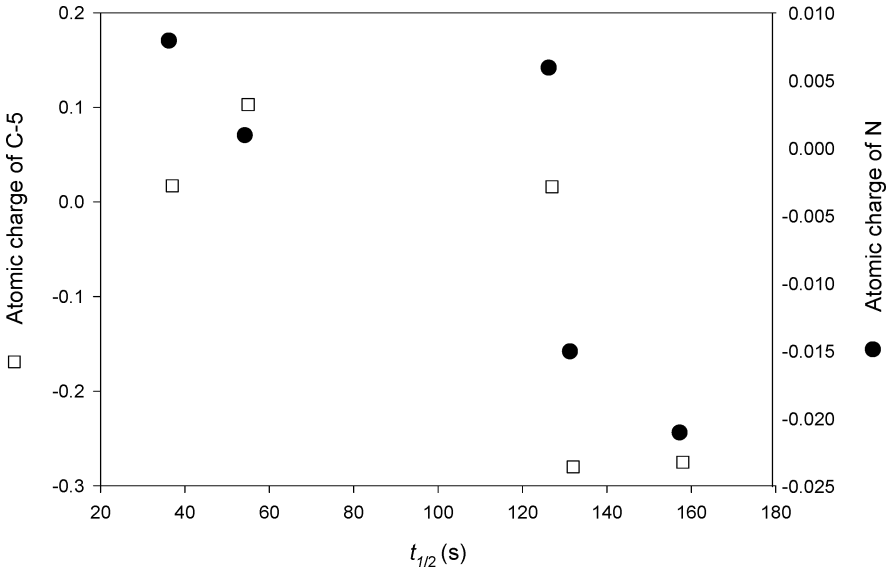

Figure 6. Plots of atomic charges on C-5 and nitronyl-N from the Natural Population Analysis at the HF/6-31G* level vs the half-lives of various •OH adducts.

TABLE 5: First-Order Approximation of Half-Lives of •OH Adducts[a]

adduct	$k_1/10^5$ s^{-1}	k_2[adduct]$_o/10^4$ s^{-1}	$t_{1/2}$/min
DMPO/•OH	20.1 ± 1.8	4.4 ± 1.7	55 (61.2 ± 5.9)[b]
EMPO/•OH	9.13 ± 0.7	8.4 ± 0.6	127
BocMPO/•OH	33.3 ± 1.4	5.6 ± 0.8	37
DEPMPO/•OH	8.77 ± 0.7	9.2 ± 1.3	132
DIPPMPO/•OH	7.29 ± 0.8	13.6 ± 0.9	158

[a] Based on the first-order rate constant; values are the mean average of three to five measurements. [b] Ref 26.

previously reported[26] $t_{1/2}$ of 61.2 ± 5.9 min for the DMPO/•OH adduct is within the experimental error of the value of 55 min determined from our studies. The BocMPO/•OH adduct gave the shortest $t_{1/2}$ = 37 min compared to $t_{1/2}$ > 2 h for the EMPO/•OH, DEMPO/•OH, and DIPPMPO/•OH adducts, with DIPPMPO/•OH being the longest-lived •OH adduct with $t_{1/2} \approx$ 2.5 h. A half-life of 116(7) min was reported for 4-carboxy-3,3,5,5-tetramethyl-1-pyrroline *N*-oxide[26] **6**.

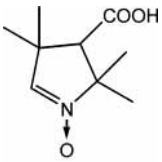

6

Interestingly, from Table 4 and Figure 6, a general trend can be observed in the magnitude of atomic charges based on the B3LYP/6-31G*//HF/6-31G* level of calculation. In general, charges on N and C-5 are significantly more negative for phosphorylated spin adducts compared to those for the rest of the •OH adducts. In the case of DMPO/•OH adducts, a highly positive charge on C-5 has been predicted. However, calculations show that there is no significant difference in the atomic charge of C-2 for all of the spin adducts, and there is relatively less negative charge on the O in phosphorylated nitrones compared to that on the other •OH adducts. These patterns in the atomic charges for various spin adducts suggest that the unimolecular decomposition of spin adducts can be influenced by relatively high positive charges on both N and C-5, considering that the atomic charges on C-2 and O are not significantly different. One exception to this is the BocMPO/•OH adduct, which has similar electronic properties to the EMPO/•OH adduct but with a half-life that is 3-fold shorter than that of EMPO/•OH.

Also worth noting is the behavior of the formation and decay of diastereomeric carboxylated •OH adducts. Spectra shown in Figure 3 are highly reproducible and show that the rates of formation and decay of cis and trans •OH adducts for both EMPO and BocMPO vary considerably. Although the formation of cis and trans •OH adducts in carboxylated nitrones is energetically favorable as shown in Table 3, the relative stability of these adducts, varies greatly and correlates with differences in their electronic properties. Thus, as shown in Table 4, charges on nitronyl-N, C-2, and C-5 are more positive for the more stable cis configuration, whereas nitronyl-O is more negative.

Conclusions

Hydroxyl radical trapping by DMPO is significantly slower compared to the trapping rate of spin traps EMPO, BocMPO, DEPMPO, and DIPPMPO, whereas the half-lives of •OH adducts such as EMPO/•OH, DEPMPO/•OH, and DIPPMPO/•OH are significantly longer compared to those of the DMPO/•OH and BocMPO/•OH adducts. These results are consistent with theoretical calculations indicating that •OH reactivity toward nitrones can be affected partially by the presence of electron-withdrawing alkoxycarbonyl and dialkoxyphosphoryl substituents. Moreover, the relative magnitude of atomic charges on nitronyl-N, -O, C-2, and C-5 as well as the presence of intramolecular H-bonding may provide reasonable predictions of the stability of the formed spin adduct. This approach of correlating the experimentally measured kinetics with a theoretical analysis of the spin-trapping process by nitrones could be useful in the future design of more efficient nitrones with long-lived spin adducts for various applications.

Acknowledgment. We thank The Ohio Supercomputer Center (OSC) for supporting this research, Professor James Fishbein of the Chemistry Department, University of Maryland, Baltimore County, for access to his synthesis lab, and Dr. Yuanmu Deng for his assistance in computer programming. This work was supported by NIH grants HL38324, HL63744, and HL65608. C.M.H. acknowledges support from the NSF-Funded Environmental Molecular Science Institute at the Ohio State University (CHE-0089147).

Supporting Information Available: Energies of theoretically optimized structures of nitrones and spin adducts at the B3LYP/6-31G*//HF/6-31G level. This material is available free of charge via the Internet at http://pubs.acs.org.

References and Notes

(1) Rojas Wahl, R. U.; Zeng, L.; Madison, S. A.; DePinto, R. L.; Shay, B. J. *J. Chem. Soc., Perkin Trans. 2* **1998**, 2009.

(2) Jenkins, C. A.; Murphy, D. M.; Rowlands, C. C.; Egerton, T. A. *J. Chem. Soc., Perkin Trans. 2* **1997**, 2479.

(3) Santos, C. X. C.; Anjos, E. I.; Ohara, A. *Arch. Biochem. Biophys.* **1999**, *372*, 285.

(4) Hawkins, C. L.; Davies, M. J. *Free Radical Biol. Med.* **1998**, *24*, 1396.

(5) Misik, V.; Reisz, P. *Ultrason. Sonochem.* **1996**, *3*, S173.

(6) Stolze, K.; Udilova, N.; Nohl, H. *Free Radical Biol. Med.* **2000**, *29*, 1005.

(7) Dikalov, S. I.; Mason, R. P. *Free Radical Biol. Med.* **2001**, *30*, 187.

(8) Lai, C.; Piette, L. H. *Biochem. Biophys. Res. Commun.* **1977**, *78*, 51.

(9) Zhang, L.-Y.; Stone, K.; Pryor, W. A. *Free Radical Biol. Med.* **1995**, *19*, 161.

(10) Ma, Z.; Zhao, B.; Yuan, Z. *Anal. Chim. Acta* **1999**, *389*, 213.

(11) Gianni, L.; Zweier, J.; Levy, A.; Myers, C. E. *J. Biol. Chem.* **1985**, *260*, 6820.

(12) Sankarapandi, S.; Zweier, J. *J. Biol. Chem.* **1999**, *274*, 34576.

(13) Zweier, J. L.; Kuppusamy, P.; Lutty, G. A. *Proc. Natl. Acad. Sci. U.S.A.* **1988**, *85*, 4046.

(14) Zweier, J. L.; Kuppusamy, P.; Williams, R.; Rayburn, B. K.; Smith, D.; Weisfeldt, M. L.; Flaherty, J. T. *J. Biol. Chem.* **1989**, *264*, 18890.

(15) Zweier, J. L.; Flaherty, J. T.; Weisfeldt, M. L. *Proc. Natl. Acad. Sci. U.S.A.* **1987**, *84*, 1404.

(16) Lai, C.; Piette, L. H. *Biochem. Biophys. Res. Commun.* **1977**, *78*, 51.

(17) Roberfroid, M.; Calderon, P. B. *Free Radicals and Oxidation Phenomena in Biological Systems*; Marcel Dekker: New York, 1995.

(18) Halliwell, B.; Gutteridge, J. M. C. *Free Radicals in Biology and Medicine*; Oxford Univeristy Press: Oxford, U.K., 1999.

(19) Bilenko, M. V. *Ischemia and Reperfusion of Various Organs: Injury, Mechanisms, Methods of Prevention and Treatment*; Nova Science Pub. Inc.: Huntington, N.Y., 2001.

(20) Rizzi, C.; Lauricella, R.; Tuccio, B.; Bouteiller, J.-C.; Cerri, V.; Tordo, P. *J. Chem. Soc., Perkin Trans. 2* **1997**, 2507.

(21) Rizzi, C.; Marque, S.; Belin, F.; Bouteiller, J.-C.; Lauricella, R.; Tuccio, B.; Cerri, V.; Tordo, P. *J. Chem. Soc., Perkin Trans. 2* **1997**, 2513.

(22) Karoui, H.; Nsanzumuhire, C.; Le Moigne, F.; Tordo, P. *J. Org. Chem.* **1999**, *64*, 1471.

(23) Olive, G.; Le Moigne, F.; Mercier, A.; Rockenbauer, A.; Tordo, P. *J. Org. Chem.* **1998**, *63*, 9095.

(24) Turner, M. J.; Rosen, G. M. *J. Med. Chem.* **1986**, *29*, 2439.

(25) Tsai, P.; Pou, S.; Straus, R.; Rosen, G. M. *J. Chem. Soc., Perkin Trans. 2* **1999**, 1759.

(26) Tsai, P.; Elas, M.; Parasca, A. D.; Barth, E. D.; Mailer, C.; Halpern, H. J.; Rosen, G. M. *J. Chem. Soc., Perkin Trans. 2* **2001**, 875.

(27) Olive, G.; Mercier, A.; Le Moigne, F.; Rockenbauer, A.; Tordo, P. *Free Radical Biol. Med.* **2000**, *28*, 403.

(28) Frejaville, C.; Karoui, H.; Tuccio, B.; Le Moigne, F.; Culcasi, M.; Pietri, S.; Lauricella, R.; Tordo, P. *J. Chem. Soc., Chem. Commun.* **1994**, 1793.

(29) Frejaville, C.; Karoui, H.; Tuccio, B.; Le Moigne, F.; Culcasi, M.; Pietri, S.; Lauricella, R.; Tordo, P. *J. Med. Chem.* **1995**, *38*, 258.

(30) Zhao, H.; Joseph, J.; Zhang, H.; Karoui, H.; Kalyanaraman, B. *Free Radical Biol. Med.* **2001**, *31*, 599.

(31) Finkelstein, E.; Rosen, G. M.; Rauckman, E. J. *J. Am. Chem. Soc.* **1980**, *102*, 4995.

(32) Villamena, F.; Zweier, J. *J. Chem. Soc., Perkin Trans. 2* **2002**, 1340.

(33) Hehre, W. J.; Radom, L.; Schleyer, P. V.; Pople, J. A. *Ab Initio Molecular Orbital Theory*; Wiley & Sons: New York, 1986.

(34) Labanowski, J. W.; Andzelm, J. *Density Functional Methods in Chemistry*; Springer: New York, 1991.

(35) Parr, R. G.; Yang, W. *Density Functional Theory in Atoms and Molecules*; Oxford University Press: New York, 1989.

(36) Becke, A. D. *Phys. Rev.* **1988**, *38*, 3098.

(37) Lee, C.; Yang, W.; Parr, R. G. *Phys. Rev. B* **1988**, *37*, 785.

(38) Becke, A. D. *J. Chem. Phys.* **1993**, *98*, 1372.

(39) Frisch, M. J.; Trucks, G. W.; Schlegel, H. B.; Scuseria, G. E.; Robb, M. A.; Cheeseman, J. R.; Zakrzewski, V. G.; Montgomery, J. A., Jr.; Stratmann, R. E.; Burant, J. C.; Dapprich, S.; Millam, J. M.; Daniels, A. D.; Kudin, K. N.; Strain, M. C.; Farkas, O.; Tomasi, J.; Barone, V.; Cossi, M.; Cammi, R.; Mennucci, B.; Pomelli, C.; Adamo, C.; Clifford, S.; Ochterski, J.; Petersson, G. A.; Ayala, P. Y.; Cui, Q.; Morokuma, K.; Malick, D. K.; Rabuck, A. D.; Raghavachari, K.; Foresman, J. B.; Cioslowski, J.; Ortiz, J. V.; Stefanov, B. B.; Liu, G.; Liashenko, A.; Piskorz, P.; Komaromi, I.; Gomperts, R.; Martin, R. L.; Fox, D. J.; Keith, T.; Al-Laham, M. A.; Peng, C. Y.; Nanayakkara, A.; Gonzalez, C.; Challacombe, M.; Gill, P. M. W.; Johnson, B. G.; Chen, W.; Wong, M. W.; Andres, J. L.; Head-Gordon, M.; Replogle, E. S.; Pople, J. A. *Gaussian 98*, revision A.11.3; Gaussian, Inc.: Pittsburgh, PA, 1998.

(40) Xu, Y. K.; Chen, Z. W.; Sun, J.; Liu, K.; Chen, W.; Shi, W.; Wang, H. M.; Zhang, X. K.; Liu, Y. *J. Org. Chem.* **2002**, *67*, 7624.

(41) Villamena, F.; Zweier, J. Unpublished report, 2002.

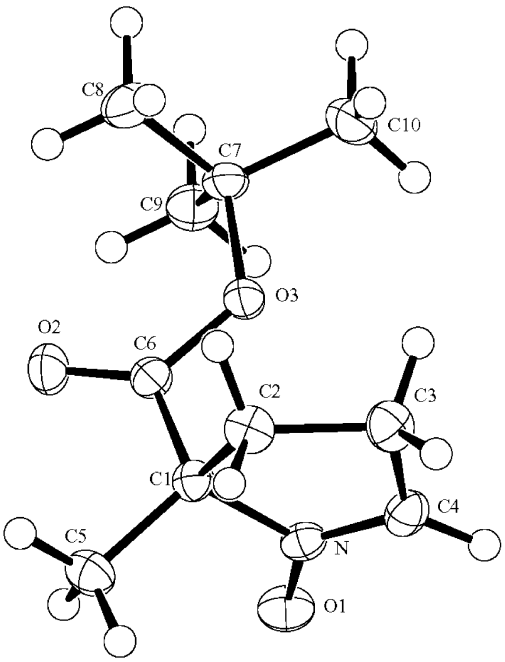

BocMPO: $C_{10}H_{17}NO_3$, monoclinic, P2(1)/n, a = 12.1985(2) Å, b = 6.2722(1) Å, c = 14.5012(3) Å, β = 107.039(1)°, 1060.81(3) Å^3; final R_1 = 0.037.

(42) Pople, J. A.; Scott, A. P.; Wong, M. W.; Radom, L. *Isr. J. Chem.* **1993**, *33*, 345.

(43) Reed, A. E.; Weinhold, F. A.; Curtiss, L. A. *Chem. Rev.* **1998**, *98*, 899. Qualitative trends should be consistent at the NPA level as has been shown by Wiberg and Rablen (*J. Comput. Chem.* **1993**, *14*, 1504).

(44) Adams, E. G.; Wardman, P. *Free Radicals Biol.* **1977**, *3*, 53.

(45) Rosen, G. M.; Britigan, B. E.; Helpern, H. J.; Pou, S. *Free Radicals: Biology and Detection by Spin Trapping*; Oxford University Press: New York, 1999.

(46) von Sonntag, C. *The Chemical Basis of Radiation Biology*; Taylor and Francis Ltd.: London, 1987.

(47) Boyd, S. L.; Boyd, R. J. *J. Phys. Chem.* **1994**, *98*, 11705.